



Contents lists available at SciVerse ScienceDirect

# Journal of Quantitative Spectroscopy & Radiative Transfer

journal homepage: [www.elsevier.com/locate/jqsrt](http://www.elsevier.com/locate/jqsrt)

## Far infrared Fourier-transform spectroscopy of mono-deuterated hydrogen peroxide HOOD

Doris Herberth<sup>a,\*</sup>, Oliver Baum<sup>a</sup>, Olivier Pirali<sup>b,c</sup>, Pascale Roy<sup>b</sup>, Sven Thorwirth<sup>a</sup>, Koichi M.T. Yamada<sup>d</sup>, Stephan Schlemmer<sup>a</sup>, Thomas F. Giesen<sup>a</sup>

<sup>a</sup> I. Physikalisches Institut, Universität zu Köln, D-50937 Köln, Germany

<sup>b</sup> Ligne AILES - Synchrotron SOLEIL, L'Orme des Merisiers, F-91192 Gif-Sur-Yvette, France

<sup>c</sup> Institut des Sciences Moléculaires, UMR 8214 CNRS - Université Paris-Sud, Bât. 210, 91405 Orsay Cedex, France

<sup>d</sup> Institute for Environmental Management Technology (EMTech), AIST Tsukuba-West, Onogawa 16-1, Tsukuba, Ibaraki 305-8569, Japan

### ARTICLE INFO

Available online 1 March 2012

#### Keywords:

Deuterated hydrogen peroxide  
Far infrared spectrum  
Internal rotation  
Torsional splitting  
AILES beamline SOLEIL

### ABSTRACT

We present the gas phase spectrum of singly deuterated hydrogen peroxide, HOOD, in its vibrational ground state, recorded by the high resolution Fourier-transform interferometer located at the AILES synchrotron beamline connected to SOLEIL. More than 1000 transitions in the range from 20 to 143  $\text{cm}^{-1}$  were assigned, leading to a set of preliminary rotational and centrifugal distortion constants determined by least squares fit analysis. All transitions are split by the tunneling motion of a hindered internal rotation. The splitting has been determined to be 5.786(13)  $\text{cm}^{-1}$  in the torsional ground state and it shows a dependence on the rotational quantum number  $K_a$ . Some perturbations were not treated yet, but the present analysis permits to obtain a preliminary set of parameters.

© 2012 Elsevier Ltd. All rights reserved.

### 1. Introduction

Hydrogen peroxide,  $\text{H}_2\text{O}_2$ , plays an important role in the chemistry of the earth's stratospheric ozone layer and has been found in the planetary atmosphere of Mars [1] and recently in the cold environment of a star forming region towards  $\rho$  Oph A [2]. As the simplest peroxide, i.e. a compound with an oxygen–oxygen single bond, it shows internal rotation motion.

The torsion–rotation spectrum of hydrogen peroxide has been studied extensively in the past. As early as 1934, Penny and Sutherland calculated the structure of  $\text{H}_2\text{O}_2$  and found the skew chain structure of  $C_2$  symmetry being the most stable [3]. Ever since then, experimental evidence has been accumulated from many sources, until in 1950 Giguere et al. [4] recorded extended infrared spectra

to obtain molecular parameters which were in agreement with the predictions made by Penny and Sutherland.

In 1993 Pelz et al. [5] reanalyzed the torsional potential of  $\text{H}_2\text{O}_2$  and calculated effective rotational constants for the ground state and the first three torsionally excited states. By fitting calculated constants to the observed values of Flaud et al. [6], the dependence of the structural parameters on the torsional angle was determined. Among others, Kuhn et al. [7] performed calculations of the electronic ground state potential energy surface of hydrogen peroxide in 1999, providing an *ab initio* value for the torsional splitting. More references to the studies of the torsion–rotation spectrum of hydrogen peroxide can be found in Camy-Peyret et al. [8].

In 2001 Bak et al. determined equilibrium structures for 19 molecules by using a least-squares fit analysis involving rotational constants from experiment and vibrational corrections from high-level electronic-structure calculations [9]. The accuracy of the results surpassed that reported in most purely experimental determinations. In case of HOOH the authors figured out significant

\* Corresponding author. Tel.: +49 221 4703483.

E-mail address: herberth@ph1.uni-koeln.de (D. Herberth).

discrepancy in structural parameters when comparing calculated and empirical structures, indeed, it was largest among the 19 studied molecules. While the mean absolute error for the bond distances of the 19 molecules was 0.09 pm in CCSD(T)/cc-pCVQZ calculations, the deviation to experimental values for  $R_{OO}$  in  $H_2O_2$  turned out to be 6 times larger. The authors claimed that this discrepancy originates from the experimental data and urged for a re-investigation of the molecule.

In the same year, Koput et al. noted the lack of precise experimental data on the hydrogen peroxide isotopomers [10]. For this purpose they calculated spectroscopic constants for  $H_2O_2$ , HOOD,  $D_2O_2$  and  $H_2^{18}O_2$  based on a high-quality *ab initio* six-dimensional potential energy surface to support a future analysis of the rotation–torsion spectra of these molecules.

In 2001 Flaud et al. succeeded in measuring the torsion rotation spectrum of doubly deuterated hydrogen peroxide,  $D_2O_2$ , from 20 to  $1200\text{ cm}^{-1}$  and determined highly accurate constants for the two torsional ground state levels [11].

To satisfy the need of precise experimental data on HOOD, we performed extensive measurements of the torsion–rotation spectrum of the molecule. Unlike  $H_2O_2$ , which possesses a  $C_2$  symmetry axis, its mono-deuterated form, HOOD, has no geometrical symmetry at all ( $C_1$ ). Despite its asymmetric structure mono-deuterated hydrogen peroxide happens to be a nearly prolate symmetric top with Ray's asymmetry parameter of  $\kappa = -0.985$ . With two different internally rotating moieties, OH and OD, HOOD represents the most general case of internal rotation in four-atomic skew-chain molecules.

Due to its internal rotation motion, HOOD is an ideal test-bed for recent quantum chemical models describing internal rotation. The molecules  $H_2S_2$  and  $H_2O_2$ , which are analogous to HOOD, but of higher symmetry, are expected to show an alternation of the size of the torsional splitting with the parity of the rotational quantum number  $K_a$  [5,13]. This kind of staggering is well explained by the model developed by Hougen [14], in which the energy splitting is expressed in terms of *cis*- and *trans*-tunneling interaction. This model was also applied to the more complicated molecule HNCNH to successfully describe its alternating torsional splitting [15].

The principal axis of HOOD corresponding to the smallest moment of inertia (*a*-axis) coincides almost with the axis between the two oxygen atoms. The OH and the OD group undergo a large amplitude motion, namely torsion, about the OO bond. Two barriers hinder this motion: a smaller one in the *trans*-configuration and a larger one in the *cis*-configuration [6]. Tunneling through the barriers causes a splitting of energy levels whose size depends on the barrier heights and the reduced-mass of the torsional motion. The splitting also – but to a smaller extend – depends on the rotational quantum numbers  $J$  and  $K_a$ . According to this, tunneling mainly through the *trans*-barrier of HOOD leads to a splitting of rotational energy levels into two sub-levels which were reported to be separated by about  $5.6\text{ cm}^{-1}$  [12]. We label these two levels as  $\nu_{LAM}=0$  and  $\nu_{LAM}=1$  in increasing energy order (LAM stands for Large Amplitude Motion, i.e. internal rotation).

Expectedly, the molecule HSOH, which unlike  $H_2S_2$ ,  $H_2O_2$  and HNCNH has no geometrical symmetry, shows a more complicated dependence of the torsional splitting

on  $K_a$ : the alternation with  $K_a$  has a periodicity of approximately three. Yamada et al. extended Hougen's model to describe this phenomenon [16]. While Hougen et al. postulated a  $4\pi$  periodicity of the torsional potential energy and the torsional wavefunctions instead of the “natural”  $2\pi$ , Yamada et al. extended the period to  $6\pi$ . Since HOOD is analogous to HSOH and thus is expected to show the same  $K_a$ -dependence of torsional splitting, it is an ideal test-bed for this new model.

In this work, we report the first preliminary molecular parameters for the ground state and the value for the torsional splitting as well as its dependence on  $K_a$  for the HOOD molecule. In order to confirm the assignments, which are required to perform advanced studies to determine the torsional potential function, the transition frequencies have been analyzed in the present study, as the first step, employing the Watson-type effective Hamiltonian for each tunneling doublet component.

## 2. Experimental aspects

The spectra of HOOD were recorded at the SOLEIL Synchrotron facility in France during 15 shifts of beam time at the AILES beamline, making use of a Bruker IFS 125 Fourier Transform Infrared Spectrometer. The beam-line properties and the application to high resolution gas-phase spectroscopy are described in details in Refs. [18–20]. For the studies of HOOD two spectra were recorded at  $0.0011\text{ cm}^{-1}$  resolution. The first spectrum recorded in the  $30\text{--}600\text{ cm}^{-1}$  range was obtained by averaging 400 scans. For this measurement a 4.2 K cooled bolometer detector, a  $6\text{ }\mu\text{m}$  thick mylar beamsplitter, and a 2 mm thick polyethylene cold filter were used. The iris aperture at the entrance of the interferometer was set at 12.5 mm and the scanner velocity was 80 kHz.

The second spectrum recorded in the  $15\text{--}50\text{ cm}^{-1}$  range is the average of 120 scans. It was obtained using a 1.6 K bolometer combined with the  $6\text{ }\mu\text{m}$  thick mylar beamsplitter and the scanner velocity set at 20 kHz. For this measurement, the storage ring was operating in the “hybrid mode” corresponding to filling 3/4 of the ring with 400 electron bunches (accounting for a current of 390 mA) while the last 1/4 ring was filled with a single 10 mA bunch. This bunch emits very intense but unstable coherent FIR radiation whose emission peaks around  $15\text{ cm}^{-1}$  (see [21]). In order to limit the noise in this spectrum, we spatially filtered the coherent radiation using the entrance iris set to 5 mm aperture.

Deuterated hydrogen peroxide was prepared following a method described by Flaud et al. [11]. A 30% dilute solution of hydrogen peroxide in water was mixed with the same amount of  $D_2O$ . To increase the concentration of HOOD in the sample, the water and its isotopologues were slowly evaporated at reduced pressure and at a temperature of about  $40\text{ }^\circ\text{C}$  until the volume of the sample was reduced to about two-thirds. Due to the exchange reaction of D- and H-atoms, the resulting solution contained  $H_2O_2$ , HOOD and  $D_2O_2$  with a statistical ratio of 1:2:1 at an optimal condition, as well as  $H_2O$ , HDO and  $D_2O$  with the same ratio. In order to improve the sensitivity, the gas sample was introduced into a long path 40 m White-type

multi-reflection cell with a base-line length between the optics of 1 m and thus a total of 39 reflections in the cell. The sample gas was continuously injected into the cell, maintaining a slow and constant flow at a total pressure of about 1 mbar.

The resulting spectrum was obtained by averaging 552 single spectra with an overall integration time of about 25 hours. Transition frequencies were calibrated using accurate FIR water lines reported by Matsushima et al. [22].

### 3. Data analysis

#### 3.1. Assignments and fits

As an almost accidental symmetric rotor HOOD shows characteristic  ${}^rQ_{K_a}$  branches ( $\Delta K_a = +1$ ,  $\Delta J = 0$ ) at

frequencies of approximately  $(A - (B + C)/2)(2K_a + 1)$ , with  $K_a = 0, 1, 2, \dots$ , which exhibit a noticeable accumulation of lines in a relatively small frequency region and thus allow for the unambiguous identification of the torsion-rotational lines. Therefore, in the first step of the analysis, the  ${}^rQ$  branches of HOOD were assigned with the help of *ab initio* calculations of the molecular constants [10].

Fig. 1 gives an overview over the  $Q$  branch structure in the frequency region of  $20\text{--}80\text{ cm}^{-1}$ . For the sake of simplicity, in this figure only the  $Q$  branch transitions are shown. In the upper trace, the *Fortrat*-diagram is displayed, depicting the rotational quantum number  $J$  of the lower state as a function of the transition frequency. Green:  $\nu''_{\text{LAM}} = 1$ . Blue:  $\nu''_{\text{LAM}} = 0$ . The branches with high intensity represent the transitions between the two torsional states, while the low intensity transitions centered between them are the

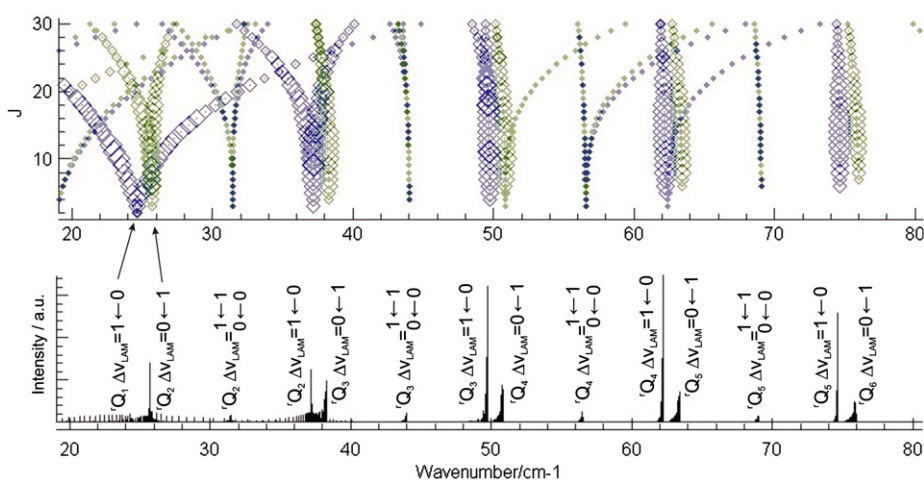


**Fig. 1.** Overview over the  $Q$  branch structure of the spectrum of HOOD between  $20$  and  $80\text{ cm}^{-1}$ . The spectrum was derived by least squares fit analysis of 1400 assigned transitions. In the *Fortrat*-diagram in the upper trace,  $J$  of the lower state is shown as a function of the transition frequency, the size of the points symbolizing the intensity of the corresponding transition. Green:  $\nu''_{\text{LAM}} = 1$ . Blue:  $\nu''_{\text{LAM}} = 0$ . The branches with high intensity include transitions between the two torsional states, while the low intensity transitions centered between them take place within one torsional state. (For interpretation of the references to color in this figure legend, the reader is referred to the web version of this article.)

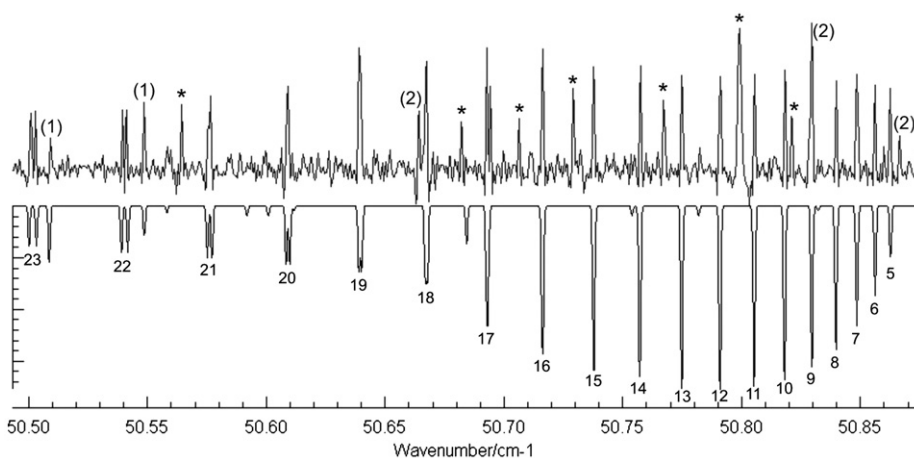


**Fig. 2.** Band head of the  ${}^rQ_4$ -branch ( $\nu''_{\text{LAM}} = 0 \leftarrow \nu''_{\text{LAM}} = 1$ ) of HOOD. The experimental spectrum recorded at the SOLEIL-AILES beamline is depicted in the upper trace, while in the lower trace a calculated spectrum based on the molecular parameters of the data analysis is plotted. (1)  $R$ - and  $P$ -branch transitions of HOOD, (2) transitions of  $\text{H}_2\text{O}_2$ , \* unassigned lines.

transitions within one torsional state. The transitions of  $\Delta K_a > 1$  are too weak to be identified. The lines of each  $Q$  branch further split into two asymmetry components due to the inertial asymmetry. They are clearly seen in the Fortrat-diagram, especially in the  $Q$  branches with low  $K_a$ .

Figs. 2 and 3 give a closer view of the band origins of the  ${}^rQ_4$  branches with  $\nu_{\text{LAM}} = 0 \leftarrow 1$  and  $\nu_{\text{LAM}} = 1 \leftarrow 0$ . The comparison of the observed and simulated spectra indicates the high quality of the fit.

Once a sufficient number of  $Q$  branch transitions were assigned, the resulting spectroscopic parameters allowed for the prediction of  $P$  and  $R$  branch transition frequencies. In total, more than 1000 transitions of the molecule were assigned to the vibrational ground state in the frequency range of 20–143  $\text{cm}^{-1}$  up to  $J=30$  and  $K_a=8$ , as listed in Table 1.

Based on the structural *ab initio* parameters of  $\text{H}_2\text{O}_2$  [10] we calculated the dipole moments of HOOD with the help of the software *Gaussian03* [23] at MP3/cc-pVTZ level of theory. The resulting dipole moments are  $\mu_a = 0.0458$  D,  $\mu_b = 0.5593$  D and  $\mu_c = 1.7252$  D. Thus, the rotational spectrum of HOOD should show  $b$ -type transitions in addition to about 10 times stronger  $c$ -type transitions, and also very weak  $a$ -type transitions. We assigned  $b$ -type transitions, within one torsional level  $\nu_{\text{LAM}} = 0$  or  $\nu_{\text{LAM}} = 1$ , i.e. pure-rotational transitions, while the assigned  $c$ -type transitions involved a change of the torsional state. Since  $\mu_a$  is 10 times weaker than the  $\mu_b$ , no  $a$ -type transitions could be observed. We compared the intensity of several  $b$ - and  $c$ -type  $Q$  branch transitions with the same  $J$ , and found that the observed intensity ratio is in accordance with the theoretically expected ratio of  $\mu_c^2/\mu_b^2 = 9.5$ .

Colin Western's software PGOPHER [24] was used for the least squares fitting, employing a standard Watson type Hamiltonian in  $S$  reduction. The two torsional components  $\nu_{\text{LAM}} = 0$  and  $\nu_{\text{LAM}} = 1$  were treated as two separated states. The preliminary obtained molecular constants suggest that there should be an avoided level crossing between the  $K_a=1$  level of  $\nu_{\text{LAM}} = 0$  and 1. A similar avoided crossing was observed in HSOH for  $K_a=2$  [25].

**Table 1**Maximum values of  $J$  observed in each branch.

$K_a''$	$\nu_{\text{LAM}} = 1 \leftarrow 0$			$\nu_{\text{LAM}} = 0 \leftarrow 1$			$\nu_{\text{LAM}} = 0 \leftarrow 0$	$\nu_{\text{LAM}} = 1 \leftarrow 1$
	${}^rP$	${}^rQ$	${}^rR$	${}^rP$	${}^rQ$	${}^rP$	${}^rQ$	${}^rQ$
0	–	–	12	–	–	–	–	–
1	–	–	–	–	–	–	–	–
2	–	16	11	10	–	–	12	12
3	12	11	13	–	16	15	10	14
4	20	24	16	13	26	22	19	16
5	26	30	26	19	29	18	19	22
6	21	20	20	19	30	25	20	24
7	24	27	23	19	21	18	18	22
8	19	22	19	–	14	12	20	17

**Table 2**Experimentally determined effective molecular constants of HOOD for the ground vibrational state in MHz. Uncertainties in parentheses are  $1\sigma$  from the least square fit in units of the last quoted digit.

Parameter	$\nu_{\text{LAM}} = 0$	$\nu_{\text{LAM}} = 1$
Origin	0.0	173 457.99(395)
A	212 839.985(402)	212 667.410(409)
B	24 872.00(145)	24 815.888(406)
C	23 374.75(153)	23 445.372(444)
$D_K$	6.9058(125)	6.7631(111)
$D_{JK}$	0.99792(320)	0.99166(286)
$D_J$	0.078429(390)	0.077822(309)
$d_1$	–0.01303(544)	0.00415(162)
$d_2$	–0.029593(539)	–0.010673(700)
$H_K \times 10^3$	1.899(109)	1.6058(931)
$H_{KJ} \times 10^3$	1.9033(754)	1.0977(565)
$H_{JK} \times 10^3$	–0.0600(143)	–0.03330(690)
$H_J \times 10^3$	–0.005175(526)	–0.002006(449)
$h_1 \times 10^6$	43.65(561)	5.86(288)
$h_2 \times 10^6$	14.11(283)	–47.38(482)
$h_3 \times 10^6$	0.960(196)	4.135(265)
$L_{KKJ} \times 10^6$	–11.884(674)	–7.317(461)
$L_{JK} \times 10^6$	–3.005(121)	–0.8994(797)
$L_{JJ} \times 10^6$	0.1555(108)	0.02077(655)
$L_J \times 10^6$	–0.002558(505)	0.0 (fixed)

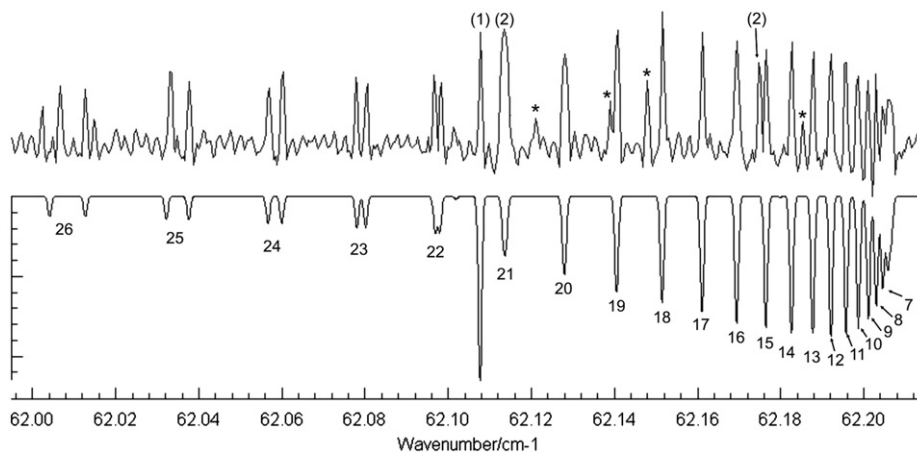


**Fig. 3.** Band head of the  ${}^rQ_4$ -branch ( $\nu_{\text{LAM}} = 1 \leftarrow \nu_{\text{LAM}} = 0$ ) of HOOD. The experimental spectrum recorded at the SOLEIL-AILES beamline is depicted in the upper trace, while in the lower trace a calculated spectrum based on the molecular parameters of the data analysis is plotted. (1)  $R$  and  $P$  branch transitions of HOOD, (2) transitions of  $\text{D}_2\text{O}_2$ , \* unassigned lines.

Since a global analysis requires additional interaction terms to the standard Watson type rotational Hamiltonian, the lines possibly perturbed by the interaction were not included in our least squares fit. Thus, effective spectroscopic constants were derived solely on the basis of unperturbed or less-perturbed lines. Due to the high accuracy of the measurements all five quartic centrifugal distortion constants, seven sextic constants as well as  $L_{KJ}$ ,  $L_{JK}$ ,  $L_{JK}$ , and  $L_J$  were determined and are given in Table 2. Among the parameters listed there,  $d_1$  and  $h_1$  are less precisely determined by the fit. If both of them are kept fixed to 0 we obtain slightly larger RMS deviation of the fit, i.e.  $0.00040 \text{ cm}^{-1}$ . If we add the parameter  $d_1$ , the RMS deviation is improved to  $0.00038 \text{ cm}^{-1}$ . By adjusting both  $d_1$  and  $h_1$ , it is further improved to be  $0.00036 \text{ cm}^{-1}$ , which is very close, in our opinion, to the experimental uncertainty of  $10^{-4} \text{ cm}^{-1}$ .

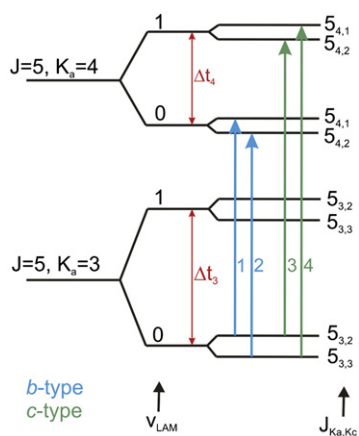


**Fig. 4.** A schematic of the torsional energy splitting caused by the *trans*-barrier. The size of the splitting was determined with the help of a combination of *b*-type transitions within a torsional state and *c*-type transitions between the two torsional states. In this example, the torsional splitting for  $J=5$ ,  $K_a=4$  is derived using the transitions (1) to (4) by calculating the average value of the differences (4)–(2) and (3)–(1).

### 3.2. Torsional splitting

From the observed *b*-type and *c*-type transitions the torsional splitting for each  $(J, K_a)$  level can be determined, as illustrated in Fig. 4. For such cases, the rotational dependence of the tunneling splitting is shown in Fig. 5. From the fit results, the torsional splitting at the  $(J, K_a)=(0,0)$  limit is determined to be  $5.786(13) \text{ cm}^{-1}$  in the ground torsional state. The splitting determined in the present study agrees very well with the experimental value ( $5.8 \text{ cm}^{-1}$ ) reported by Kuhn et al. [7] as a preliminary value, but is larger than the calculated value ( $4.9 \text{ cm}^{-1}$ ) of Koput et al. [10]. The tunnel splitting for each  $K_a$  at the  $J=0$  limit can be obtained from the effective spectroscopic parameters by employing the symmetric-top approximation. The decrease of the torsional splitting with increasing  $K_a$  was observed as shown in Fig. 6. Similar effects were also observed in  $\text{H}_2\text{O}_2$ ,  $\text{D}_2\text{O}_2$ , as well as in the molecule  $\text{HNCNH}$  as reported by Jabs et al. [15].

### 3.3. Avoided crossing

We observed resonant interactions between the energy levels of same symmetry (parity). Although HOOD has only  $C_1$  point group symmetry, the torsion–rotation wavefunctions of the quantum states must be symmetric (+ parity) or anti-symmetric (– parity) by inverting the signs of all coordinates of the atoms. Fig. 7 shows the energy level diagram of HOOD for the levels with  $K_a=0$  and 1. The energy region is of special interest, because several levels of same symmetry happen to lie nearby. The symmetry is indicated by *e* (parity= $(-1)^J$ ) and *f* (parity= $-(-1)^J$ ) following the recommended notation [26]. For example the levels  $K_a=0$ ,  $\nu_{\text{LAM}}=1$ , which is of *f* symmetry, and the *f*-component of  $K_a=1$ ,  $\nu_{\text{LAM}}=0$  show near resonances in the region of approximately  $J=0$  to  $J=10$ . Strong resonances and even an avoided crossing of levels can be expected for

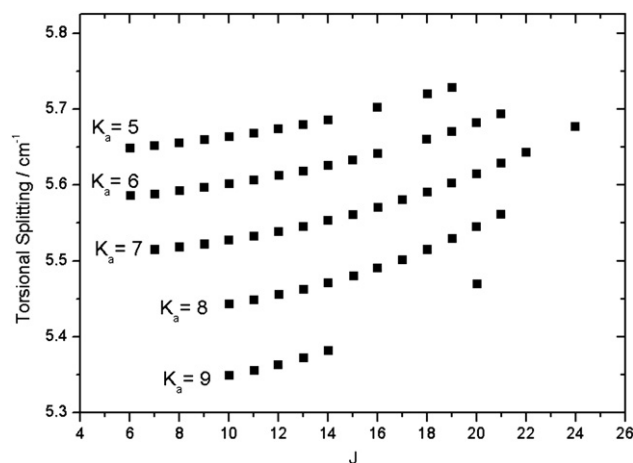


**Fig. 5.** Measured torsional splitting due to the *trans*-barrier for HOOD as a function of rotation quantum numbers  $J$  and  $K_a$ .

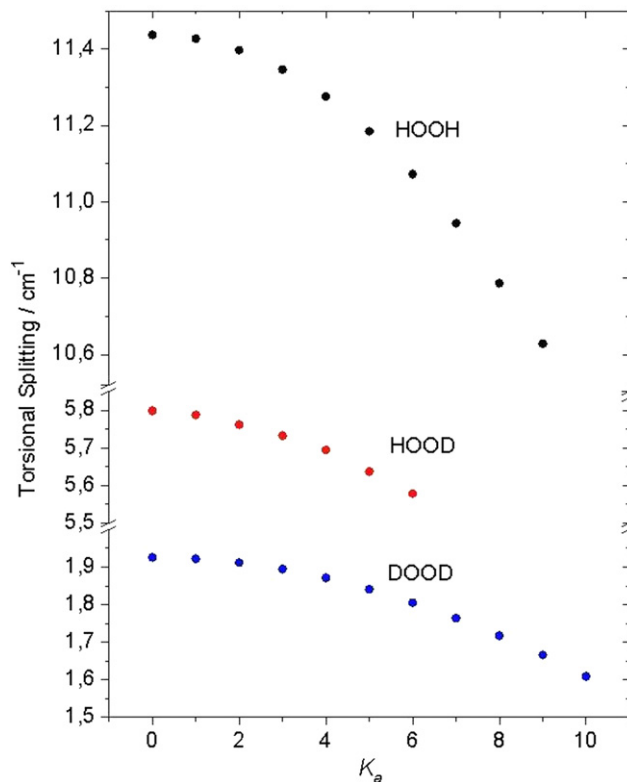


**Fig. 6.** Torsional splitting due to the *trans*-barrier for H<sub>2</sub>O<sub>2</sub>, HOOD and D<sub>2</sub>O<sub>2</sub> as a function of  $K_a$ . The splittings at the  $J=0$  limit were calculated on the basis of experimental rotational constants by Flaud et al. (D<sub>2</sub>O<sub>2</sub>) [11] and Camy-Peyret et al. (H<sub>2</sub>O<sub>2</sub>) [8] and from our experimentally determined constants for HOOD.

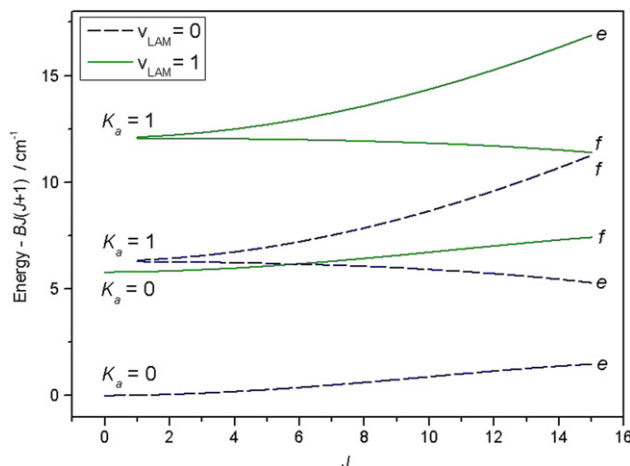


**Fig. 7.** Energy level diagram of HOOD. The lines illustrate the location of the energy levels extrapolated from least squares fit analysis. Due to resonances between the energy levels of same symmetry *e* and *f*, no transitions could be assigned definitely in the  $K_a=0, \nu_{LAM}=1$  and  $K_a=1, \nu_{LAM}=0$  levels, nor in the lower asymmetry component of the level  $K_a=1, \nu_{LAM}=1$ .

the *f*-components of  $K_a=1, \nu_{LAM}=0$  and  $K_a=1, \nu_{LAM}=1$ , which actually would cross in the region of  $J=15$ . Because of the perturbations, so far no lines could be assigned for the transitions which involve the levels  $K_a=0, \nu_{LAM}=1$  and  $K_a=1, \nu_{LAM}=0$ . We are currently working on an extended analysis including the perturbations, which will be published in an additional paper.

#### 4. Conclusions

The gas phase spectrum of HOOD was measured from 15 to 700  $\text{cm}^{-1}$  and more than 1000 transitions could be assigned in the 20–143  $\text{cm}^{-1}$  range. On the basis of these measurements we derived preliminary effective rotational constants for the molecule (see Table 2).



Because of the observed resonances for the energy levels with  $K_a=0$  and 1 (Fig. 7), which leads to a breakdown of the standard Watson type Hamiltonian, we solely used unperturbed and less-perturbed transitions for the derivation of rotational constants. The size of the torsional splitting in the ground vibrational state of HOOD is revised by the present study to be  $5.786(13) \text{ cm}^{-1}$ . The staggering of the splitting as a function of  $K_a$  with a period of three, expected for HOOD in analogy of HSOH, was not observed. This is due to the very low *trans*-barrier compared to the *cis*-barrier in hydrogen peroxide: the splitting is caused almost solely by the *trans*-tunneling.

The size of the torsional splitting increases with the rotational quantum number  $J$ , as can be seen in Fig. 5. In contrast, the size of the torsional splitting decreases with increasing  $K_a$  (see also Fig. 5). This phenomenon was also observed in other molecules, e.g.  $\text{H}_2\text{O}_2$ ,  $\text{H}_2\text{S}_2$  [5] and HNCNH [15], and may be caused by a change of the OOH- and OOD-angles, which – due to increasing centrifugal forces – shift from their equilibrium value in HOOD of  $99.9^\circ$  [10] towards the  $90^\circ$  position. This leads to a higher effective potential and consequently to a smaller torsional splitting with increasing  $K_a$ .

## Acknowledgements

This work has been financially supported by the Deutsche Forschungsgemeinschaft (DFG) via research grant GI319/2-1. In addition, S. Thorwirth acknowledges funding by the Deutsche Forschungsgemeinschaft through grant TH 1301/3-1. Beamtime was allocated under project 20090856.

## References

- [1] Encrenaz T, Bezard B, Greathouse TK, Richter MJ, Lacy JH, Atreya SK, et al. Hydrogen peroxide on Mars: evidence for spatial and seasonal variations. *Icarus* 2004;170:424–9.
- [2] Bergman P, Parise B, Liseau R, Larsson B, Olofsson H, Menten KM, et al. Detection of interstellar hydrogen peroxide. *Astron Astrophys* 2011;531:L8.
- [3] Penny WG, Sutherland GBBM. The theory of the structure of hydrogen peroxide and hydrazine. *J Chem Phys* 1934;2:492–8.
- [4] Giguere PA. The infra-red spectrum of hydrogen peroxide. *J Chem Phys* 1950;18:88–92.
- [5] Pelz G, Yamada KMT, Winnewisser G. Torsional dependence of the effective rotational constants of  $\text{H}_2\text{O}_2$  and  $\text{H}_2\text{S}_2$ . *J Mol Spectrosc* 1993;159:507–20.
- [6] Flaud JM, Camy-Peyret C. The far infrared spectrum of  $\text{H}_2\text{O}_2$ . First observation of the staggering of the levels and determination of the *cis* barrier. *J Chem Phys* 1989;91:1504–10.
- [7] Kuhn B, Rizzo TR, Luckhaus D, Quack M, Suhm MA. A new six-dimensional analytical potential up to chemically significant energies for the electronic ground state of hydrogen peroxide. *J Chem Phys* 1999;111:2565–87.
- [8] Camy-Peyret C, Flaud JM, Johns LWC, Noël M. Torsion–vibration interaction in  $\text{H}_2\text{O}_2$ : first high-resolution observation of  $\nu_3^1$ . *J Mol Spectrosc* 1992;155:84–104.
- [9] Bak KL, Gauss J, Jørgensen P, Olsen J, Helgaker T, Stanton JF. The accurate determination of molecular equilibrium structures. *J Chem Phys* 2001;114:6548–56.
- [10] Koput J, Carter S, Handy NC. Ab initio prediction of the vibrational–rotational energy levels of hydrogen peroxide and its isotopomers. *J Chem Phys* 2001;115:8345–50.
- [11] Flaud JM, Johns JWC, Lu Z, Winnewisser G, Klein H. The torsion–rotation spectrum of  $\text{D}_2\text{O}_2$ . *Can J Phys* 2001;79:367–74.
- [12] Fehrensen B, Luckhaus D, Quack M. Mode selective stereomutation tunnelling in hydrogen peroxide isotopomers. *Chem Phys Lett* 1999;300:312–20.
- [13] Winnewisser G, Yamada KMT. Millimetre, submillimetre and infrared spectra of disulphane (HSSH) and its isotopic species. *Vib Spectrosc* 1991;1:263–72.
- [14] Hougen JT. Summary of group theoretical results for microwave and infrared studies of  $\text{H}_2\text{O}_2$ . *Can J Phys* 1984;62:1392–402.
- [15] Jabs W, Winnewisser M, Belov SP, Klaus T, Winnewisser G. The  $\nu_{Q_1}$  branch of carbodiimide, HNCNH, at 1.1 THz. *Chem Phys* 1997;225:77–91.
- [16] Yamada KMT, Winnewisser G, Jensen P. Internal rotation tunnelling in HSOH. *J Mol Structure* 2004;695–696:323–37.
- [17] Brubach JB, Manceron L, Rouzières M, Piralì O, Balcon D, Kwabia Tchana F, et al. AIP conference proceedings, vol. 1214; 2010. p. 81–4.
- [18] Cuisset A, Nanobashvili L, Smirnova I, Bocquet R, Hindle F, Mouret G, et al. *Chem Phys Lett* 2010;492:30–4.
- [19] McKellar ARW. *J Mol Spectrosc* 2010;262:1–10.
- [20] Barros J, Manceron L, Brubach JB, Creff G, Evain C, Couprie ME, et al. *J Phys: Conf Ser (JPCS)*, Proc WIRMS, in press.
- [21] Matsushima F, Tomatsu N, Nagai T, Moriwaki Y, Takagi K. *J Mol Spectrosc* 2006;235:190–5.
- [22] Frisch MJ, Trucks GW, Schlegel HB, Scuseria GE, Robb MA, Cheeseman JR, et al. Gaussian 03, revision B.03. Pittsburgh, PA: Gaussian, Inc.; 2003.
- [23] Western CM. PGOPHER. Release 7.0.101. University of Bristol, <<http://pgopher.chm.bris.ac.uk>>; 2010.
- [24] Ross SC, Yamada KMT, Itoc F. Torsion–rotation coupling and the determination of the torsional potential energy function of HSOH. *Phys Chem Chem Phys* 2010;12:11133–50.
- [25] Brown JM, Hougen JT, Huber KP, Johns JWC, Kopp I, Lefebvre-Brion H, et al. The labeling of parity doublet levels in linear molecules. *J Mol Spectrosc* 1975;55:500–3.